Journal of Controlled Release 319 (2020) 371–381

Contents lists available at ScienceDirect

Journal of Controlled Release

journal homepage: www.elsevier.com/locate/jconrel

Natural IgM dominates *in vivo* performance of liposomes

Tianhao Ding[a,1], Juan Guan[a,b,1], Mengke Wang[b], Qianqian Long[c], Xia Liu[d], Jun Qian[b], Xiaoli Wei[a], Weiyue Lu[b], Changyou Zhan[a,b,*]

[a] Department of Pharmacology, School of Basic Medical Sciences & State Key Laboratory of Molecular Engineering of Polymers, Fudan University, Shanghai 200032, PR China
[b] School of Pharmacy, Fudan University & Key Laboratory of Smart Drug Delivery (Fudan University), Ministry of Education, Shanghai 201203, PR China
[c] Department of medical oncology, Fudan University Shanghai Cancer Center & Department of Oncology, Shanghai Medical College, Fudan University, Shanghai 200032, China
[d] Department of Neurology, Shanghai Pudong Hospital, Fudan University Pudong Medical Center, Shanghai 201399, PR China

ARTICLE INFO

Keywords:
Liposome
IgM
Plasma protein
in vivo performance
Complement activation

ABSTRACT

Prevalent deposition of plasma proteins on nano-surface alters the synthetic identity of liposomes in blood circulation. The key plasma protein(s) that can dominate *in vivo* fate of liposomes are of central importance for preclinical design and precise medication of liposome-based therapeutics. Herein, natural IgM, but not IgG, is identified to ubiquitously absorb on liposomal surface and takes the lead in complement activation of different species. The absorbed natural IgM, which negatively correlates with the *in vivo* performance of liposomes, becomes a potential indicator to guide the *de novo* design and optimization of liposomes. More importantly, the varying natural IgM levels in cancer patients may be one of the causal factors for clinical differences in response to liposome-based therapeutics. Clinical monitoring of the natural IgM level and its binding with liposomes becomes crucial to optimize the therapeutic regimen prior to the application of liposome-based therapeutics.

1. Introduction

During the past several decades, liposomes have been extensively exploited as a class of versatile carrier for the delivery of anti-cancer and anti-infection therapeutics [1–3]. Many efforts have been made to understand the physical and biological characteristics of such biocompatible and surface-tunable lipid vesicles. Substantive progress has been witnessed both in the basic research and the bench-to-bedside translation of liposomes for therapy and diagnosis purposes [4,5]. So far > 20 liposomal formulations have been approved globally for the intervention of cancers and infectious diseases [6]. The application of liposomes brings many advantages over the conventional formulations to improve efficacy and/or mitigate side effects, including sustained or controlled release of payloads, prolonged duration of therapeutic agents in blood circulation *via* PEGylation, and separation of therapeutics from healthy organs (*i.e.* doxorubicin *v.s.* heart) [7–10]. More interestingly, it is capable of achieving spatiotemporal delivery of payloads by further modulation of lipid bilayers with sensitive molecules and functionalization of liposomal surface with targeting agents [11–16]. However, both the bench-to-bedside translation and application of liposomes in the clinic are in a dilemma due to ambiguous understandings on *in vivo* delivery mechanisms.

The surface identity is crucial to the *in vivo* performance of liposomes, including pharmacokinetic profile, biodistribution, immunogenicity, targeting yield, nanotoxicity, and many others [17]. Unfortunately, vigorous interaction between liposome and biomedia is ubiquitous, making the surface identity of liposomes distinct from the synthetic one. Upon entry into the blood stream, liposomes are surrounded by heavy levels of plasma proteins, which spontaneously absorb on the nano-surface. The formation of so called “protein corona” recomposes the surface identity of liposomes and severely affects *in vivo* performance [18–22]. Such discrepancy between the synthetic and biological identities presents a wide gap in the bench-to-bedside translation of liposomes. Hundreds of plasma proteins have been reported to deposit on doxorubicin loaded liposomes (Doxil), and some of them exert significant impacts on the *in vivo* fate of liposomes [23,24]. The presence of targeting agents can alter the composition of protein corona to a great extent, making the *in vivo* performance of liposomes unpredictable [25,26]. Thus, it is urgent to identify the key plasma protein(s) and to decipher their effects on *in vivo* fate of liposomes.

* Corresponding author at: Department of Pharmacology, School of Basic Medical Sciences & State Key Laboratory of Molecular Engineering of Polymers, Fudan University, Shanghai 200032, PR China.
E-mail address: cyzhan@fudan.edu.cn (C. Zhan).
[1] These authors contributed to this work equally.

https://doi.org/10.1016/j.jconrel.2020.01.018
Received 6 November 2019; Received in revised form 30 December 2019; Accepted 8 January 2020
Available online 09 January 2020
0168-3659/ © 2020 Elsevier B.V. All rights reserved.

More importantly, clinical application of the approved liposome-based therapeutics also suffers a plight. In patients, the content and component of plasma proteins undergo dynamic changes during the progress of diseases, which may severely deteriorate the unpredictable situation of clinically used liposomes. Validation of the key plasma protein(s) that dominate the *in vivo* performance of liposomes and interrogation of their regulatory mechanisms are useful to guide precise medication of liposomes in the clinic.

In the present study, liposomes with different synthetic identities are prepared and the composition of the formed protein corona is characterized in different species. Natural immunoglobulin M (IgM) ubiquitously deposits on the surface of all liposomes. The potential has been analyzed of natural IgM as an indicator to guide *de novo* design and optimization of liposomes. The clinical relevance of these findings has been investigated by evaluating the binding with liposomes and complement activation as functions of the varying levels of natural IgM in cancer patients.

2. Methods

2.1. Reagents and antibodies

^{D}CDX ($G^{D}R^{D}E^{D}I^{D}R^{D}TG^{D}R^{D}A^{D}E^{D}R^{D}W^{D}S^{D}E^{D}K^{D}F$), RGD (GRGDSP), A7R (ATWLPPR), ANG (TFFYGGSRGKRNNFKTEEY) were chemically synthesized *via* Fmoc-based solid-phase peptide synthesis [27] (CS336 peptide synthesizer, CSBio (Shanghai) Ltd.). FA-PEG3400-DSPE was chemically synthesized as previously reported [28]. Mal-PEG3400-DSPE, HSPC (hydrogenated soy phosphatidylcholine) and mPEG2000-DSPE were purchased from A.V.T. Pharmaceutical, Co., Ltd. (Shanghai, China). Sephadex G50 and DiI (1,1′-dioctadecyl-3,3,3′,3′-tetramethylindocarbocyanine) were from Sigma-Aldrich (St. Louis, MO). Cholesterol was acquired from Nippon Fine Chemical, Co., Ltd. (Takasago, Japan). Goat anti-mouse IgM mu chain (HRP) (ab97230, 1:5000), goat anti-rat IgM mu chain (HRP) (ab97180, 1:5000), goat anti-rabbit IgM mu chain (HRP) (ab97195, 1:5000), goat anti-human IgM mu chain (HRP) (ab97205, 1:5000), rabbit polyclonal CD31 antibody (ab28364, 1:20) and mouse monoclonal IgM (ab18400), mouse IgG (ab188776), mouse complement C5a ELISA kit (ab193718), human complement C5a ELISA kit (ab193695), were from Abcam (Cambridge, MA). 3,3′,5,5’-Tetramethylbenzidine (TMB) chromogen solution for ELISA assay, DAPI (4′,6-diamidino-2-phenylindole), fast silver stain kit and SDS-PAGE sample loading buffer (5×) were purchased from Beyotime Biotechnology (Jiangsu, China). Gradient precast polyacrylamide gels (4–20%) (Cat# 456–1093) and protein dual color standards (Cat# 1610374) were from BIO-RAD (Hercules, CA). Doxorubicin hydrochloride and daunorubicin hydrochloride were purchased from Dalian Meilun Biotechnology Co., Ltd. (Dalian China).

2.2. Cell line, animals and human serum

Neuro-2a cell line was from the Type Culture Collection of Chinese Academy of Sciences (Shanghai, China). Adult male BALB/c mice, Sprague–Dawley rats, New Zealand rabbits and SCID (Severe combined immunodeficiency) mice were acquired from Shanghai SLAC Laboratory Animal Co., LTD (Shanghai, China) and kept under SPF condition. All animal experiments were carried out in accordance with guidelines evaluated and approved by the ethics committee of Fudan University. The use of human serum in this study was approved by the Ethics Committee of the Fudan University Shanghai Cancer Center and informed consent was obtained from each health donor and cancer patient.

2.3. Preparation of peptide-PEG3400-DSPE

Peptides (^{D}CDX, RGD, A7R, ANG) containing an additional cysteine were conjugated with Mal-PEG3400-DSPE *via* sulfhydryl-maleimide coupling method [29]. Mal-PEG3400-DSPE (50 mg) was dissolved in chloroform and evaporated to form a thin film, then dried for 2 h under vacuum and hydrated with ultrapure water (UPW, 5 ml) at 37 °C. Thiolated peptide was dissolved in 2 ml UPW and mixed with Mal-PEG3400-DSPE micelle (peptide: Mal-PEG3400-DSPE = 1.5: 1, molar ratio), then 0.1 M phosphate-buffered solution (pH = 7.4, 3 ml) was added in the mixture to react for 6 h at room temperature under magnetic stirring. The mixture was placed in a dialysis bag with the molecular weight cutoff (MWCO) of 8000–14,000 Da in UPW for 48 h to remove any residual free peptides and salts. All peptide modified lipids were freeze-dried for further use.

2.4. Preparation and characterization of liposomes

Plain PEGylated liposomes (sLip) were prepared by the thin film hydration and extrusion method [30]. A mixture of HSPC/cholesterol/mPEG-DSPE (molar ratio of 52:43:5) were dissolved in chloroform and vacuum-rotary evaporated to form a thin film, then dried overnight under vacuum. The dried lipid film was hydrated with saline at 60 °C. The lipid dispersion was extruded through polycarbonate membranes with pore diameters of 200 nm and 100 nm. For the conventional liposomes (Lip, without PEGylation), HSPC and cholesterol (55:45) were dissolved in chloroform to form the thin film. Other populations of liposomes containing different molar ratio of targeting ligand modified PEG3400-DSPE were prepared following the same methods except for the addition of 0.5%, 1% and 2% targeting ligand-PEG3400-DSPE before the formation of thin film (the molar ratios of mPEG2000-DSPE were decreased to 4.5%, 4% and 3%, respectively). DiI-loaded liposomes were prepared by adding 0.5% molar ratio of DiI before the formation of lipid thin film. Doxorubicin-loaded liposomes were prepared using ammonium sulfate gradient method [31]. Briefly, the dried lipid film was hydrated with 0.32 M ammonium sulfate at 60 °C. The lipid dispersion was extruded through polycarbonate membranes with pore diameters of 200 nm and 100 nm, and the external phase was replaced with saline by Sephadex G50 column. Doxorubicin hydrochloride (DOX) was added into liposomes (DOX/lipid, mass ratio 1:10) and the mixture was incubated at 60 °C for 20 min, then free doxorubicin was removed by G50 column. Lipid concentration was measured using phosphorus assay [32] and DOX concentration was measured by reversed-phase high performance liquid chromatography (HPLC). The size and zeta-potential of liposomes were measured in deionized water at a lipid concentration of 0.5 mM using ZetasizerNano ZS90 (Malven Instrument, southborough, MA).

2.5. Characterization of protein corona

Whole blood was collected from BALB/c mice, SD rats and rabbits, and kept at room temperature for 30 min and centrifuged at 1000 × *g* to collect the serum. One hundred microliters liposomes (containing 8 mM HSPC) were incubated with the same volume of serum in low protein binding tubes at 37 °C for 1 h, then 800 μL chilled phosphate buffered saline (PBS) was added and centrifuged at 14,000 × *g* for 30 min. The pellets were rinsed with chilled PBS (300 μL) thrice under the same condition and re-suspended in a solution containing 30 μL PBS, 7.5 μL SDS-PAGE sample loading buffer (5×) and 2 μL β-mercaptethanol. Protein aliquots were separated by size on a 4%–20% gradient polyacrylamide gel and transferred to PVDF membrane. Nonspecific binding sites on PVDF membrane were blocked by incubation in PBST (PBS plus 0.1% Tween 20) containing 5% dry skimmed milk at room temperature for 1 h, followed by incubation overnight at 4 °C with goat anti-mouse, rat or rabbit IgM antibody conjugated with horseradish peroxidase. The signal was imaged (ChemiScope 6000, Clinx Co. Ltd) and the data was analyzed by Image J software (see supplementary Fig. 7a, 8, 9, 10 and 11).

BALB/c mice were intravenously injected *via* the tail vein with DiI loaded liposomes (50 mg HSPC per kg of mice) and anesthetized at 1 h.

Blood was sampled and the serum was collected after centrifugation at 1000 ×*g*. The fluorescence intensity of serum was measured by fluorescence detector to quantify the concentration of DiI loaded liposomes (Ex at 550 nm and Em at 570 nm). The liposome-protein complex was collected and measured following the same methods as aforementioned except that the loading quantity of protein sample was quantified by the concentration of DiI loaded liposomes (see supplementary Fig. 7b).

2.6. Neuro-2a cell culture and bioactivity of ^{D}CDX on liposomal surface

Neuro-2a cells were cultured in DMEM medium containing 10% FBS, 100 units/mL penicillin and 100 μg/mL streptomycin with 5% CO_2 at 37 °C. Cells were harvested after trypsinization and suspended in chilled PBS (1×10^6 cells in 270 μL PBS). DiI loaded liposomes with different modification degree of ^{D}CDX (lipid concentration 10 mg mL^{-1}) pre-incubated with the equal volume (15 μL) of either fresh BALB/c mouse serum or PBS for 1 h at 37 °C were added. After incubation overnight, cells were centrifuged at 130 × *g* and rinsed with chilled PBS (1 mL) thrice. DiI positive cells were counted using flow cytometry.

2.7. Pharmacokinetic studies

SD rats (23 mg HSPC per kg of rats), BALB/c mice (50 mg HSPC per kg of mice) and New Zealand rabbits (12 mg HSPC per kg of rabbits) were intravenously injected with DiI loaded liposomes. At predominated time points, blood was sampled and plasma was separated by centrifugation at 1000 × *g* for 10 min. The plasma concentration of liposomes was detected by a fluorescence spectrophotometer (Ex at 550 nm and Em at 570 nm).

To study the accelerated blood clearance (ABC) phenomena, SD rats were intravenously injected a low dose of liposomes without DiI loading (2.3 mg HSPC per kg of rats). After 5 days, the pretreated rats were intravenously injected with DiI labeled liposomes (23 mg HSPC per kg of rats) and plasma was collected after centrifugation at 1000 × *g* for 10 min. Plasma concentration of DiI after the second injection was studied as aforementioned. Anti-PEG IgM titration in SD rat plasma (collected before the second injection) was detected by ELISA assay.

The pharmacokinetic profile of loaded doxorubicin in different populations of liposomes was also studied in SD rats after intravenous injection (2 mg DOX per kg of rats). Blood was sampled at 5 min, 15 min, 30 min, 1 h, 2 h, 4 h, 8 h, 12 h and 24 h post injection. Plasma was separated by centrifugation at 1000 × *g* for 10 min, and 50 μL plasma was mixed with 50 μL UPW, 100 μL methanol (containing 10 μg/mL daunomycin as the internal standard) and 400 μL chloroform to extract DOX. After 1 min vortex and 15 min centrifugation at 8000 × *g*, the chloroform phase was transferred into a new tube and dried overnight. Samples were re-dissolved in 30% acetonitrile and DOX was measured after centrifuged at 12000 × *g* for 8 min by reversed-phase HPLC coupled with a fluorescence detector (Ex at 480 nm and Em at 550 nm).

2.8. C5a quantification

Mouse serum was collected from BALB/c and SCID mice and stored at −80 °C. Human serum was collected from cancer patients and healthy donors with informed consent. IgM depleted serum was obtained by incubation with 0.2 M β-mercaptoethanol at 37 °C for an hour. For reconstitution, mouse IgG and mouse IgM were added to depleted serum or SCID serum. Liposomes (containing 8 mM HSPC) were incubated with normal, depleted or reconstituted serum at 37 °C for 40 min. Complement activation end-product C5a in serum was determined using mouse or human complement C5a ELISA kit according to manufacturer's instructions.

2.9. Immunogenicity of the liposomes

BALB/c mice were intraperitoneal injected four doses (by weekly, 50 mg HSPC per kg of mice) of liposomes. Blood was sampled 7 days after the fourth injection and kept at room temperature for 30 min. Serum was collected after centrifugation at 1000 × *g* for 10 min and stored at -80 °C. Anti-PEG IgM / IgG titrations in BALB/c serum were detected by ELISA assay using mPEG-DSPE (sLip) or ^{D}CDX-PEG-DSPE (0.5%^{D}CDX-sLip, 1% ^{D}CDX-sLip and 2% ^{D}CDX-sLip) as antigens.

2.10. ELISA assay

High binding 96-well ELISA plates were coated with 2 μg mPEG-DSPE or ^{D}CDX-PEG-DSPE per well for immunogenicity studies, or liposomes containing 20 μg HSPC per well for the studies on natural IgM absorption. All wells were rinsed with PBST thrice and blocked with 3% BSA at 37 °C for 1 h. Serum was gradually diluted with PBS and incubated in the microtiter wells at 37 °C for 1 h. After rinses with PBST thrice and blocking with 3% BSA at 37 °C for 30 min, horseradish peroxidase labeled goat anti-IgM or IgG antibody was added to react with IgM or IgG at 37 °C for 1 h. TMB (3,3′,5,5′-Tetramethylbenzidine) was added for 5–15 min and 0.18 M sulfuric acid was used to terminate the reaction. UV absorbance at 450 nm was measured.

2.11. Biodistribution study

To quantify the brain distribution of different populations of liposomes in healthy BALB/c mice, DiI-loaded Liposomes were intravenously injected *via* the tail vein (50 mg HSPC per kg of mice). At 4 h and 8 h after injection, the main organs were dissected and the brains were fixed in 4% paraformaldehyde solution overnight and anhydrated in 30% sucrose solution for 48 h. After cryostat sectioned with 16 μm thickness, the brain slices were stained with anti-CD31 antibody and DAPI, then visualized using a confocal microscope. The DiI positive areas were calculated using the Image Pro software.

Liver and spleen dissected at 4 h and 8 h after injection were weighted and transferred into a 2 ml tube and 5% triton-X 100 (10 mL 5% triton-X 100 per gram organ) was added. The tissues were smashed by a tissue grinder and the fluorescence intensity of tissue homogenates was detected by a fluorescence spectrophotometer (Ex 550 nm/Em 570 nm).

2.12. Statistical analysis

Data are means ± standard deviations (SDs) and analyzed by Student's *t*-test with GraphPad Prism software 6.0.4. $p < .05$ was considered statistically significant (N.S.: $p > .05$, $0.01 < *p < .05$, $0.001 < **p < .01$, $***p < .001$).

3. Results

3.1. Dose-effect relationship between natural IgM and ^{D}CDX modified liposomes

^{D}CDX peptide is a stable D-peptide brain targeting ligand by recognition of nicotinic acetylcholine receptors (nAChRs) expressed on the brain capillary endothelial cells [33,34]. In our previous reports [35,36], natural IgM was prone to depositing on the surface of ^{D}CDX peptide modified liposomes *via* electrostatic interaction, demonstrating negative regulatory effects on the immunocompatibility of liposomes. To investigate if any “dose-effect” relationship, we modulated the natural IgM deposition on liposomal surface by regulating the modification degree of ^{D}CDX peptide (supplementary table 1). High modification degree resulted in high zeta-potential, which may be attributed to the positive charges in ^{D}CDX peptide. Meanwhile, modification degree of ^{D}CDX did not alter the size of liposomes after extrusion through

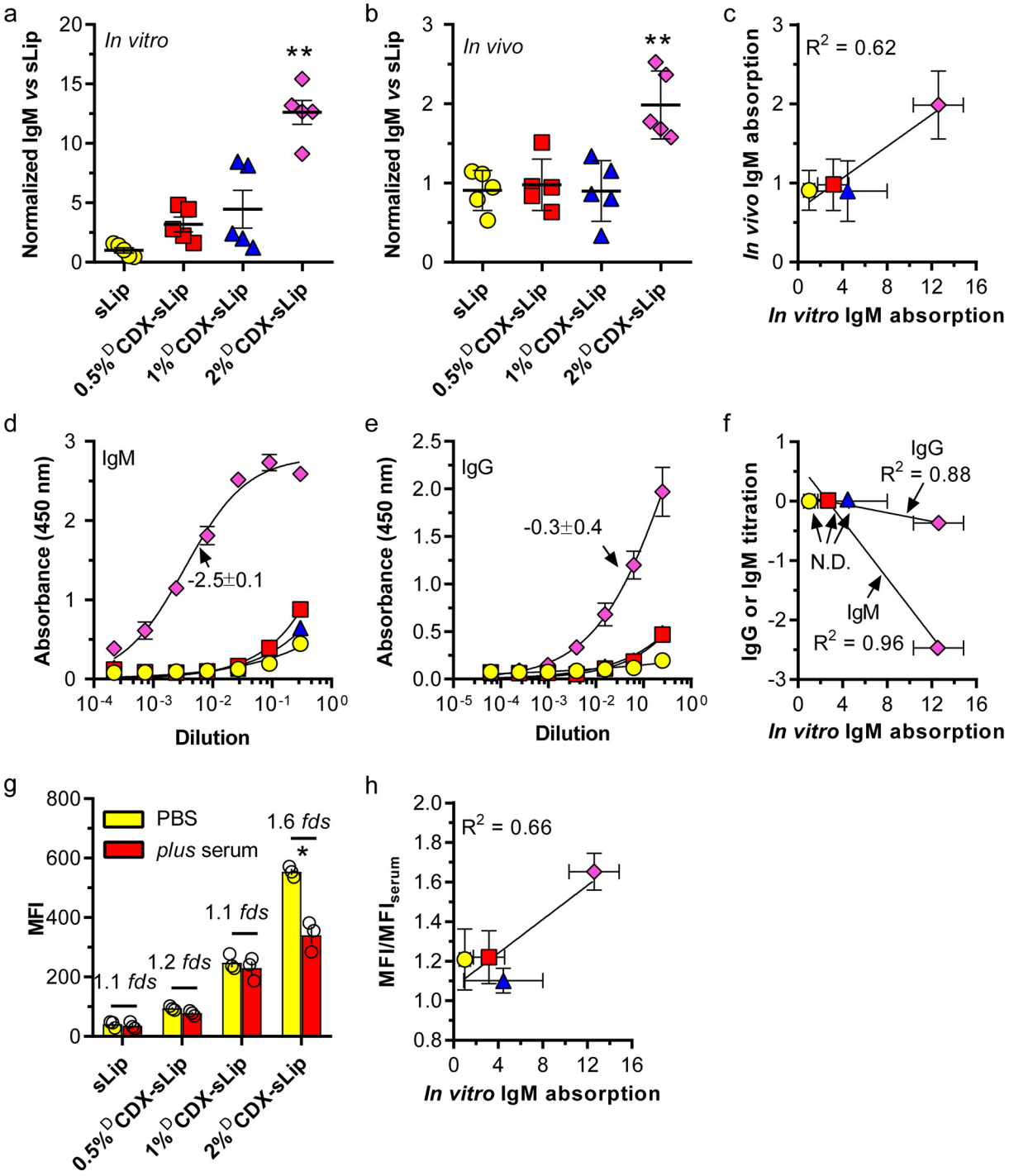

Fig. 1. Effect of ^{D}CDX modification on natural IgM absorption and the performance of liposomes. Natural IgM absorption on liposomal surface *in vitro* (a) and *in vivo* (b). Protein coronas were separated from liposomes after 1 h incubation with the equal volume of BALB/c mouse serum or 4 h after intravenous injection, and quantified by western blot assay, $n = 5$. (c) Correlation between *in vitro* and *in vivo* natural IgM absorption. Specific IgM (d) and IgG (e) titrations after four sequential doses (by weekly) of corresponding liposomes, $n = 3$. Titration was calculated as $\log(K_d)$ using the embedded equation of specific binding in GraphPad Prism 6.0. (f) Effect of *in vitro* natural IgM absorption on immunogenicity. N.D. indicates non-detectable and the titration was set as 0. (g) Effect of serum on ^{D}CDX bioactivity ($n = 3$), and (h) correlation between *in vitro* natural IgM absorption and the decrease of ^{D}CDX activity after pre-incubation with BALB/c mouse serum. Yellow, red, blue and purple circles indicate sLip, 0.5%^{D}CDX-sLip, 1%^{D}CDX-sLip and 2%^{D}CDX-sLip, respectively. Data are means ± SDs and analyzed with GraphPad Prism 6.0. * $p < .05$, ** $p < .01$ by student's *t*-test. (For interpretation of the references to color in this figure legend, the reader is referred to the web version of this article.)

membranes of predetermined sizes (see Methods).

To study the effect of ^{D}CDX modification degree on the composition of protein corona, all liposomes were incubated with the equal volume of fresh BALB/c mouse serum for 1 h at 37 °C. The formed protein coronas were collected by centrifugation and rinsed with chilled phosphate buffered saline (PBS). Natural IgM was quantified using western blot assay (Fig. 1a and supplementary Fig. 1a). Low modification degrees of ^{D}CDX (0.5% and 1%) slightly enhanced the deposition of natural IgM compared to sLip (PEGylated liposomes without ^{D}CDX modification). However, 2% ^{D}CDX modification resulted in a sharp increase (12.6 folds in comparison to that of sLip) of natural IgM absorption. The deposition of natural IgM on liposomal surface was also

studied *in vivo*. Protein coronas were collected at 4 h after intravenous injection (see Methods), and the content of IgM was quantified (Fig. 1b and supplementary Fig. 1b). Only 2%^{D}CDX-sLip showed significant enhancement of natural IgM deposition in comparison to sLip. Natural IgM absorption *in vitro* and *in vivo* demonstrated similar tendency (Fig. 1c), suggesting *in vitro* determination could reflect the *in vivo* IgM absorption.

2%^{D}CDX-sLip exhibited significant immunogenicity in our previous report [35]. Since ^{D}CDX modification degree severely affected the absorption of natural IgM, lower modification degrees of ^{D}CDX may result in improved immunocompatibility. Here the immunogenicity of different populations of liposomes was evaluated in BALB/c mice. IgG and IgM antibodies were detected after four sequential injections of liposomes (by weekly, 50 mg HSPC per kg of mice) using ELISA assay (see Methods). As shown in Fig. 1d and e, only 2%^{D}CDX-sLip generated detectable anti-^{D}CDX-PEG3400-DSPE IgG and IgM, indicating lower modification degree of ^{D}CDX could successfully mitigate the immunogenicity of liposomes. The effect of natural IgM absorption on immunogenicity was fitted (Fig. 1f), where antibody titration was quantitated as the Log(K_d) value using the embedded equation of specific binding in GraphPad Prism 6.0 and non-detectable immunogenicity was set as 0. High absorption of natural IgM in 2%^{D}CDX-sLip became the causal factor of the elevated immunogenicity. The binding affinity of ^{D}CDX on liposomal surface was evaluated using neuro-2a cells that overexpress nAChRs (receptors for ^{D}CDX peptide). As shown in Fig. 1g, higher modification degree of ^{D}CDX resulted in higher binding with neuro-2a cells, suggesting that the function of ^{D}CDX on liposomal surface was preserved to some extent. However, pre-incubation with BALB/c mouse serum slightly affected binding of sLip, 0.5%^{D}CDX-sLip and 1%^{D}CDX-sLip with neuro-2a cells, demonstrating 1.1–1.2 folds decrease of the mean fluorescence intensity. In contrast, 2%^{D}CDX-sLip displayed a sharp decrease (1.6 folds) in neuro-2a cell binding after pre-incubation with BALB/c mouse serum. The effect of BALB/c mouse serum on ^{D}CDX activity was consistent with the tendency of the natural IgM absorption (Fig. 1h).

2%^{D}CDX-sLip demonstrated rapid blood clearance in our previous report, which was driven by the enhanced absorption of natural IgM [35]. To study if the pharmacokinetic profile is as a function of natural IgM absorption, different populations of liposomes were fluorescently labeled with DiI and the plasma concentration of liposomes was measured in rats at predetermined time points after intravenous injection (see Methods). As shown in Fig. 2a, 2%^{D}CDX-sLip demonstrated rapid clearance as expected. It is interesting that 1%^{D}CDX-sLip and 0.5%^{D}CDX-sLip displayed comparable pharmacokinetic profile to that of sLip, suggesting good correlation between liposome pharmacokinetic profile and natural IgM deposition.

Accelerated blood clearance (ABC) phenomenon of liposomes has been previously reported [37,38]. Animals receiving a pre-dose (relatively low dose) of PEGylated liposomes can generate anti-PEG IgM, which is peaked at 5–7 days after injection and induces rapid blood clearance of the second injection of liposomes [39,40]. To study the ABC phenomenon, SD rats were intravenously injected with a low dose of blank liposomes (without DiI labeling, sLip, 0.5%^{D}CDX-sLip, 1%^{D}CDX-sLip, or 2%^{D}CDX-sLip, 2.3 mg HSPC per kg of rats), followed by a second injection of DiI labeled liposomes (23 mg HSPC per kg of rats, see Methods) 5 days after the first injection. As shown in Fig. 2b, 0.5%^{D}CDX-sLip and 1%^{D}CDX-sLip exhibited comparable ABC phenomenon to that of sLip in rats. After a pre-dose, sLip, 0.5%^{D}CDX-sLip and 1%^{D}CDX-sLip showed 5.5–7.9 folds decrease of the AUC. In sharp contrast, 2%^{D}CDX-sLip displayed 14.4 folds decrease of the AUC in comparison to that in rats without a pre-dose of liposomes. The effect of *in vitro* natural IgM absorption on ABC phenomenon induced the AUC decrease of liposomes was shown in Fig. 2c and supplementary Fig. 2, suggestive of the correlation between them. SD rats receiving a pre-dose of sLip generated relatively low titration of anti-PEG IgM. The increase of ^{D}CDX modification degree resulted in enhancement of IgM titrations (Fig. 2d). These results were consistent with immunogenicity shown in Fig. 1f, indicating that high modification degree of ^{D}CDX was prone to initiating enhanced immunogenic response in SD rats.

3.2. Natural IgM takes the lead in complement activation

Natural immunoglobulins (such as IgG and IgM) have been recognized as efficient opsonins to activate complement, thus to accelerate blood clearance of nanocarriers and to stimulate immune response [41–44]. Although the most abundant immunoglobulin IgG is believed to be one of the primary factor that opsonize liposomes *in vivo*, IgM is a very polyreactive immunoglobulin, demonstrating 100-fold higher efficiency of opsonization than IgG [45,46]. Complement can be activated *via* three pathways: classical pathway, lectin pathway and alternative pathway [47,48]. All three pathways converge at the point factor C3. After activation, the produced C3b plays pivotal roles to cleave C5 factor to C5a and C5b-9, which are the end-products of the complement activation pathways [49,50]. Herein, C5a was selected as the indicator to evaluate complement activation.

As shown in Fig. 3a, sLip could slightly increase the C5a concentration (15.3 ng mL^{-1}) in serum in comparison to PBS (12.0 ng mL^{-1}). 2%^{D}CDX-sLip were much more efficient to activate complement, elevating the C5a concentration to 25.4 ng mL^{-1}. To understand the effect of natural IgM absorption on complement activation, SCID mouse serum lack of immunoglobulins (natural IgG and IgM were undetectable using ELISA kits) was applied (Fig. 3b). 2%^{D}CDX-sLip generated relatively lower C5a concentration in SCID mouse serum (16.4 ng mL^{-1}) than that in BALB/c mouse serum (containing the full spectrum of immunoglobulins). Supplement of mouse IgM (1 mg mL^{-1}) in the SCID mouse serum elevated the C5a concentration to 34.6 ng mL^{-1} after 2%^{D}CDX-sLip incubation, while that of mouse IgG (2 mg mL^{-1}) only slightly increased the C5a concentration to 22.5 ng mL^{-1}. The pivotal roles of natural IgM on complement activation were further studied in BALB/c mouse serum by using β-mercaptoethanol to reduce the intramolecular disulfide bonds and deactivate natural IgM [51]. Complement activation by 2%^{D}CDX-sLip could be strongly attenuated after the addition of β-mercaptoethanol (Fig. 3b), which was recovered after addition of mouse IgM (1 mg mL^{-1}). These results reveal that natural IgM is one of the most important immunoglobulins dominating complement activation of liposomes, at least partially explaining the correlation between natural IgM absorption and *in vivo* performance of liposomes.

3.3. Natural IgM absorption on liposomes is ubiquitous

To study if it is ubiquitous of the correlation between natural IgM deposition and the *in vivo* performance of liposomes, some of the most popular targeting agents (*e.g.* folic acid, RGD peptide, Angiopep-2 and A7R peptide) during the past decades were modified on the surface of PEGylated liposomes with different molar ratios [52–59] (see the characterization of liposomes in supplementary table 2). The modification degree of targeting agents was 2% molar ratio to lipids if it was not shown in the name of liposomes. Meanwhile, conventional liposomes without PEGylation (Lip) were also prepared and characterized. As shown in Fig. 4a, modification of targeting agents resulted in varying pharmacokinetic profiles of these liposomes in SD rats. Natural IgM was detected and semi-quantified using western blot assay (see Methods, supplementary Fig. 3). Natural IgM was ubiquitously deposited on the surface of all tested liposomes with a wide range of capacity. The linear regression between normalized natural IgM (supplementary Fig. 3b) and the AUC in Fig. 4a was analyzed with GraphPad Prism 6.0 (Fig. 4b). All these liposomes fitted the linear correlation (R^2 = 0.66), suggesting natural IgM a potential indicator to predict *in vivo* performance of liposomes. Among these targeting agents, folic acid (FA) and Angiopep-2 (ANG) are respective small-molecule and peptide ligand for cancer and brain targeting, both registering high natural IgM deposition after

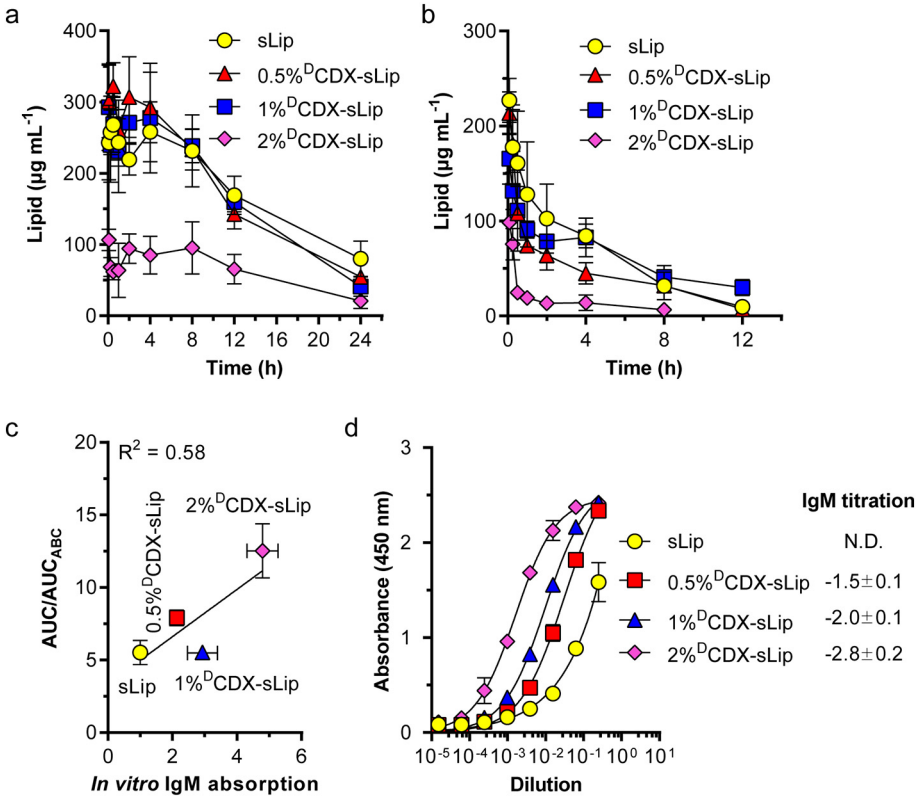

Fig. 2. Pharmacokinetic profile of liposomes as a function of natural IgM absorption in SD rats. Plasma lipid concentration curve of liposomes without (a) or with (b) pretreatment of a low dose (2.3 mg HSPC per kg of rats) of the corresponding blank liposomes (without DiI labeling) (n = 3–4). (c) Correlation between *in vitro* natural IgM absorption and the area under the curve (AUC) decrease due to the ABC phenomenon. (d) The specific IgM titration stimulated by pretreatment of a low dose of the corresponding blank liposomes (n = 3). Titration was calculated as $\log(K_d)$ using the embedded equation of specific binding in GraphPad Prism 6.0. N.D. indicates non-detectable. Data are means ± SDs and analyzed with GraphPad Prism 6.0.

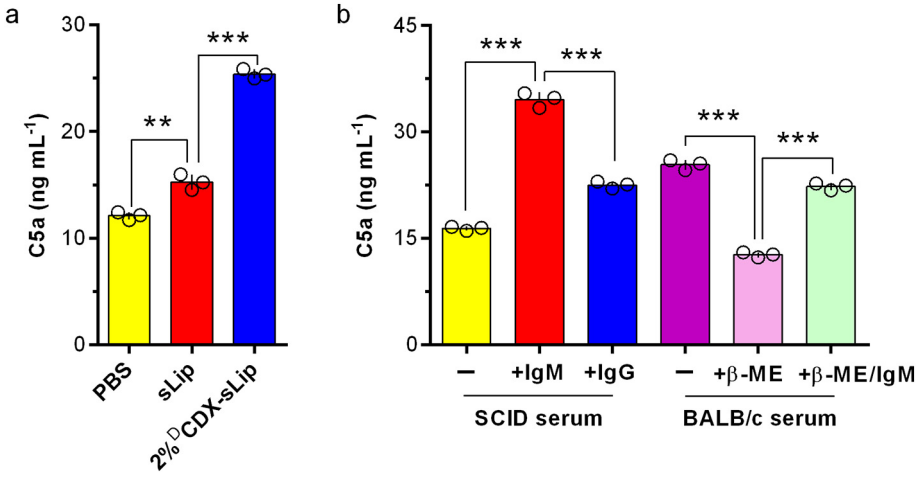

Fig. 3. Complement activation of liposomes. (a) C5a concentration in BALB/c mouse serum after incubation with PBS, sLip and 2%DCDX-sLip. (b) C5a concentration in SCID mouse serum or BALB/c mouse serum with different pre-treatments after incubation with 2%DCDX-sLip. β-ME indicates β-mercaptoethanol that can break the intramolecular disulfides of natural IgM. Data are means ± SDs (n = 3) and analyzed with GraphPad Prism 6.0. ** $p < .01$ and *** $p < .001$ by student's t-test.

modification on liposome surface at a molar ratio of 2% to lipids. Natural IgM deposition could be efficiently attenuated by reducing modification degree of both targeting agents. The modification of A7R (for VEGFR and NPR-1 targeting) and RGD (for integrins targeting) did not induce significant increase of natural IgM deposition even at high modification degree (2% molar ratio), demonstrating moderate pharmacokinetic profile in rats.

Besides the correlation between the pharmacokinetic profile of liposomes (lipid content was measured based on the incorporated fluorescent probe DiI), we also investigated that between the pharmacokinetic profile of liposome-encapsulating doxorubicin and natural IgM absorption (Fig. 5 and supplementary Fig. 4). Most of the doxorubicin loaded liposomes fitted the linear correlation (R^2 = 0.90) except for RGD-sLip/DOX, which exhibited very low natural IgM absorption but relatively rapid blood clearance. RGD peptide is a versatile targeting ligand to achieve specific delivery of diagnostic probes or therapeutic agents for different diseases [60–64]. There are many types of integrins expressed in endothelial cells, immune cells, and diseased cells/tissues [65–67]. The lack of specificity for a designated integrin subunit makes the *in vivo* delivery of RGD-sLip/DOX very complicated. The direct interactions between RGD and integrins in neutrophils/monocytes, resident macrophages, and endothelial cells would strongly affect the *in vivo* performance of liposomes [68–70]. Further studies are necessary to understand the interactions between RGD-sLip/DOX and a variety of cells, as well as their contributions to the leakage of encapsulated DOX and the rapid clearance of liposomes. These data also warn that protein corona is not the only factor affecting *in vivo* performance of active targeting liposomes. Natural IgM is a negative regulator for *in vivo* delivery of liposomes; however, low absorption of natural IgM does not guarantee favorable performance. As expected, both FA-sLip/DOX and ANG-sLip/DOX demonstrated heavy absorption of natural IgM and very rapid blood clearance in SD rats.

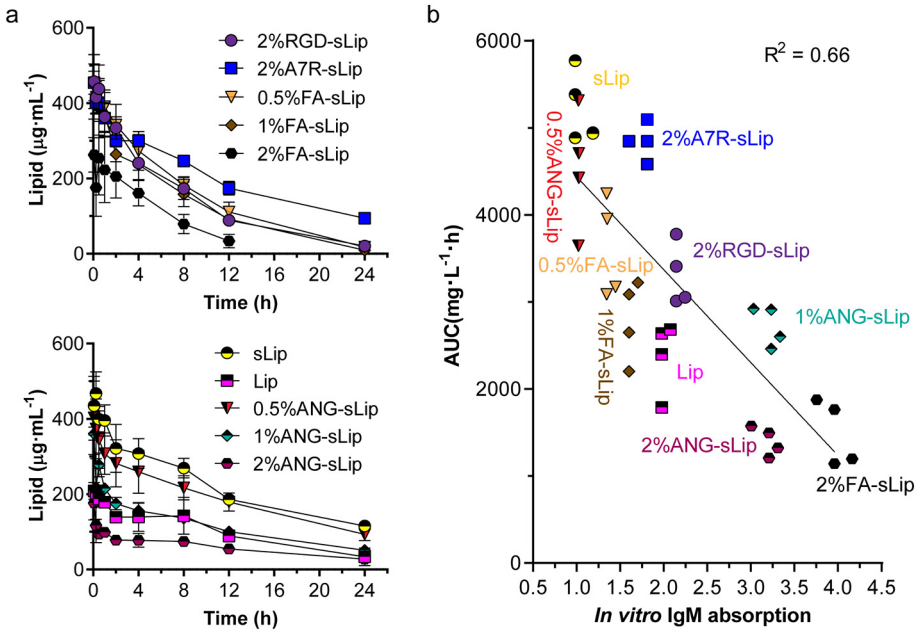

Fig. 4. Correlation between natural IgM absorption and pharmacokinetic profile of liposomes in SD rats. The percentage in the name of liposomes indicates the modification degree of targeting agents. (a) Effect of time on *in vivo* plasma lipid concentration of different liposomes after intravenous injection in SD rats. Data are means ± SDs (n = 4). (b) Linear regression between the normalized natural IgM and the area under the curve (AUC) of liposomes in SD rats. Data of each rat were staggered presented. AUC and linear regression are analyzed with GraphPad Prism 6.0.

3.4. Interspecies correlation

The source of plasma proteins has been recognized as one of the most important variables that impair the understanding of the bio-nano interfaces [71]. Interspecies transferability of the function of the key plasma proteins on *in vivo* performance of liposomes is of central importance for clinical translation [72]. Thus, the ubiquitous absorption of natural IgM and its regulatory effect on liposomes were further studied in mice and rabbits. As shown in Fig. 6 and supplementary Fig. 5, there was significant linear correlation between natural IgM deposition and *in vivo* pharmacokinetic profile of liposomes in both species (R^2 = 0.78 in mice and R^2 = 0.91 in rabbits), validating the universal regulatory role of natural IgM from different sources on the *in vivo* fate of liposomes. It is worth of noting that Lip (without PEGylation) did not well obey to the linear correlation in mice and rabbits. Lip displayed relatively low natural IgM absorption but rapid clearance in both species, indicating that PEGylation is an important factor to modulate the composition and function of the formed protein coronas on liposomal surface in some species.

Natural IgM was collected in the present study from the hard corona by centrifugation (see Methods), where binding affinity of the plasma protein is the driving force [73]. The interaction between natural IgM and liposomes was further investigated using ELISA assay (see Methods). Liposomes were immobilized on 96-well ELISA plates and incubated with serially diluted serum of mice and rabbits (see methods). As shown in Fig. 7, the binding of natural IgM demonstrated similar tendency to that in western blot assay (Fig. 6 and supplementary Fig. 5). FA-sLip, ^{D}CDX-sLip and ANG-sLip exhibited strong interaction with natural IgM of mice and rabbits; while Lip, sLip and RGD-sLip possessed low binding with natural IgM. A7R-sLip showed relatively higher binding with natural IgM from mouse serum than that from rabbit serum, which was also consistent with that in the western blot assay (Fig. 6 and supplementary Fig. 5). There are still no methods so far to accurately separate and reveal the whole functions of protein coronas. The SDS-PAGE and western blot assays have demonstrated capacity in our previous reports for the identification and semi-quantification of the key plasma protein (natural IgM) in the formed protein corona that regulates *in vivo* performance of liposomes [35]. Given that the preparation of protein corona is less reproducible among different researchers, ELISA provides a method to directly detect the interaction between liposomes and natural IgM. The consistency between western blot and ELISA assay suggested that binding affinity evaluation between natural IgM and liposomes might be an alternative method to predict *in vivo* performance of liposomes.

3.5. Natural IgM guides precise medication of liposomes in the clinic

In the present study, natural IgM was revealed to be ubiquitously associated with liposomes, and the content in the formed protein corona could be used to predict *in vivo* performance of liposomes to

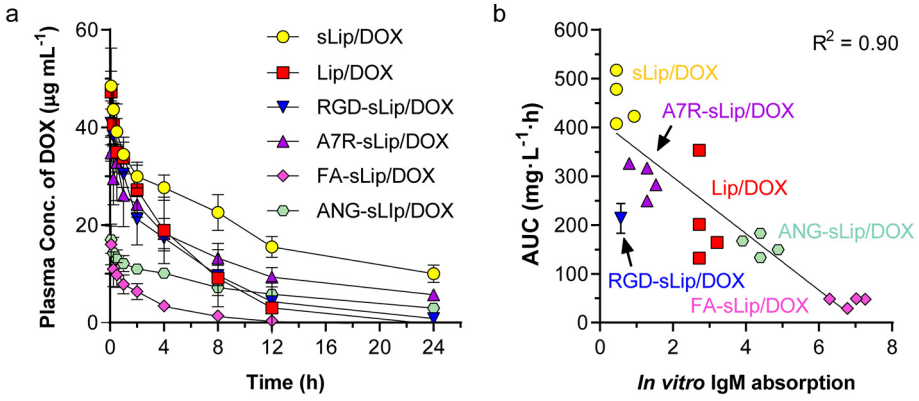

Fig. 5. Effect of natural IgM absorption on the area under the curve (AUC) of doxorubicin loaded liposomes. Modification degree of all targeting agents was 2% molar ratio to lipids. (a) The effect of time on the plasma concentration of doxorubicin. Data are means ± SDs (n = 4). (b) Linear regression between the normalized natural IgM and the area under the curve (AUC) (except for RGD-sLip/DOX) analyzed with GraphPad Prism 6.0. Data of each rat were staggered presented.

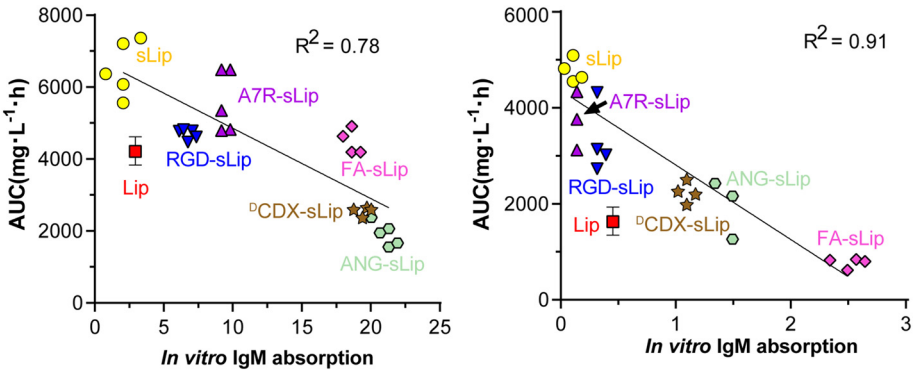

Fig. 6. Interspecies correlation. Effect of natural IgM absorption on the area under the curve (AUC) of liposomes in BALB/c mice (a)and rabbits (b) (n = 4–5). Modification degree of all targeting agents was 2% molar ratio to lipids. Data of each animal were staggered presented. AUC and linear regression are analyzed with GraphPad Prism 6.0.

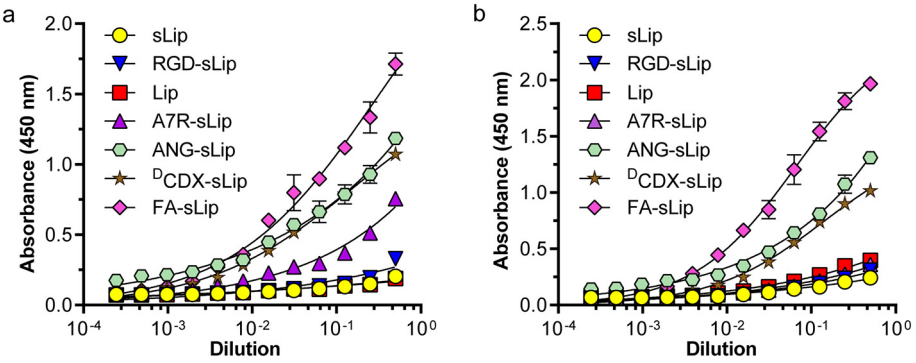

Fig. 7. Binding of natural IgM with liposomes. Serial dilutions of BALB/c mouse serum (a) or rabbit serum (b) were incubated with liposomes immobilized on 96-well ELISA plates, and the bound natural IgM was detected using anti-IgM antibody. Modification degree of all targeting ligands was 2% molar ratio to lipids. Data are means ± SD (n = 3).

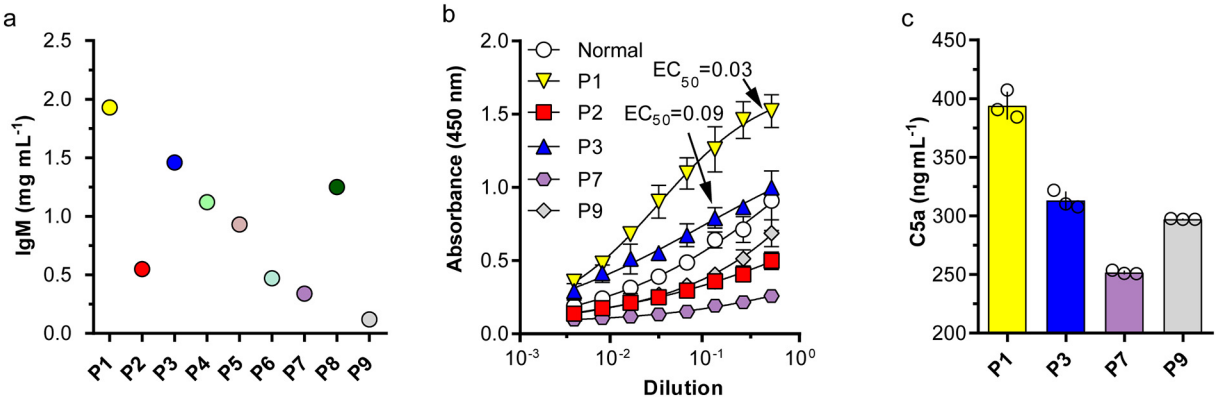

Fig. 8. Clinical relevance. (a) Quantification of natural IgM levels in cancer patients. (b) Interaction between PEGylated liposomes (sLip) and natural IgM from normal serum (Normal) or cancer patients. EC_{50} was calculated using the embedded equation of sigmoidal dose-response in GraphPad Prism 6.0. (c) C5a concentration in the serum of cancer patients after incubation with sLip. Data are means ± SD (n = 3).

some extent. Heavy absorption of natural IgM normally indicated unfavorable immunocompatibility. Liposomes are among the most popular nanomedicines. However, there are significant differences in the reactions (both therapeutic efficacy and side effects) of patients after receiving liposome-based therapeutics [74,75]. Precise medication of liposomes is still an unmet clinical need. To tackle this dilemma, we analyzed the natural IgM concentration and its interaction with liposomes from different lung cancer patients. As shown in Fig. 8a, natural IgM exhibited broad distribution among those cancer patients, ranging from 1.9 mg mL^{-1} (patient #1, P1) to 0.1 mg mL^{-1} (patient #9, P9). Meanwhile, natural IgM from P1 demonstrated the highest binding with sLip in an independent ELISA assay (Fig. 8b, sLip was used as the antigen immobilized on 96-well ELISA plates, see Methods). Low content of natural IgM (such as P2, P7 and P9) showed low binding with sLip. As expected, sLip could readily trigger complement activation in the serum of P1 that demonstrated high binding affinity (Fig. 8c) with liposomes. Interestingly, binding avidity (Fig. 8b) of natural IgM with sLip demonstrated higher consistency with complement activation (Fig. 8c) than the abundance of natural IgM in serum (Fig. 8a). For instance, the content of natural IgM from patient #9 (P9) was the lowest among all tested samples. However, its binding avidity with sLip was higher than that from patient #2 (P2) and #7 (P7). Thus, sLip in P9 exhibited enhanced complement activation in comparison to that in P7.

Varying levels and binding avidity with liposomes of natural IgM in cancer patients might be a causal factor for individual differences in response to the application of liposome-based therapeutics. High binding avidity of patient's IgM leads to significant complement activation. It is not difficult to imagine that liposomes would demonstrate distinct *in vivo* performance in these cancer patients. For example, infusion reaction that relates to complement activation is more likely to occur in Patient #1 possessing high binding avidity of natural IgM with sLip than in Patients #7 and #9. Our results suggested that natural IgM level in the cancer patient's serum and the binding avidity with liposomes may be potential indicators for clinical precise medication of

liposome-based therapeutics.

4. Discussion

As soon as liposomes enter the body and contact with blood stream, they are surrounded by heavy levels of plasma proteins and other biomolecules, which absorb on the liposomal surface. The formed protein corona alters the biological identity of liposomes, determining the interactions with organisms [76]. Comprehensive analysis on the composition and functions of protein corona has gained increasing attention during the past decade; however, it remains challenging due to technical difficulties. Protein corona is a sensitive equilibrium between absorption and desorption of plasma proteins, following the rule of Vroman effect [77,78]. Plasma proteins that exhibit high binding affinities with nano-surface directly absorb on liposomes to form hard corona. In contrast, soft corona is a highly dynamic and loose protein layer. Hundreds of plasma proteins have been characterized in the protein corona on liposomal surface, but little is known about their accurate functions in regulating the interactions of liposomes with organisms *in vivo* [24]. Thus, it is of central importance to validate the key plasma protein(s) that dominate the *in vivo* fate of liposomes.

The debate on separation techniques starts since the first publication of protein corona. Centrifugation used in the present study is a very common method to separate the hard corona, in which the plasma proteins are of relatively high binding affinities with liposomes in theory [79–82]. The natural immunoglobulin IgM is less abundant than IgG, but demonstrates higher binding affinity with ^{D}CDX modified liposomes in a separate ELISA assay (supplementary Fig. 6). It is consistent with the results in the western blot assay (Fig. 1a and supplementary Fig. 1a), suggesting that high binding of natural IgM with liposomes results in high deposition. Natural IgM, but not IgG, is found to ubiquitously absorb on liposomal surface, acting as a predominant factor for complement activation.

The modification of targeting ligands RGD peptide and A7R peptide at a molar ratio of 2% does not significantly alter the deposition of natural IgM. Folic acid, Angiopep-2 peptide and ^{D}CDX peptide significantly enhance the deposition of natural IgM, which can be attenuated by decreasing the modification degree. High absorption of natural IgM is readily to induce rapid blood clearance, elevated immunogenicity and loss of targeting yields of liposomes. Even though the binding mode between liposomes and natural IgM may vary among different surface identities, natural IgM still presents a predicting factor for the *de novo* design and optimization of liposomal formulations. In particular, the evaluation of binding affinity with natural IgM (such as ELISA assay in this study) may be more practical in preclinical screening and optimization of liposomes. Active targeting is of increasing scrutiny during the past decades due to its potential to achieve improved clinical outcome. Many efforts have been made to move forward this strategy for clinical translation. The present study validates that targeting ligands on liposomal surface may still effective after absorption of protein coronas. However, it remains unpredictable if the modification of targeting ligands changes the interaction between nanomedicines and organism. The immune system displays a large body of receptors and/or antigens that may scavenge the circulated liposomes and induce unexpected accumulation in healthy organs. The studies on *in vivo* delivery mechanism of such active targeting nanomedicines become critical for clinical translation. In addition, it is of importance to understand the effects of modification degree of targeting ligands and the encapsulated drugs on *in vivo* delivery process.

Our results also demonstrate high clinical relevance. Natural IgM in cancer patients can efficiently facilitate complement activation of clinically used liposomes (such as DOXIL) in a concentration-dependent manner. Varying levels of natural IgM in cancer patients due to immune disorders may explain the individual difference in response to liposome-based therapeutics. Natural IgM is very potential to be an indicator to guide precise medication of liposomes in the clinic. In other words, clinical monitoring of the natural IgM level becomes crucial to optimize the therapeutic regimen prior to the treatment of liposomes.

Date availability

The data that support the findings of this study are available within the paper and the supplementary information. All other data are available from the authors upon reasonable request.

Author contributions

C.Z. conceived and designed the research. T.D., J.G., M.W., Q.L., X.L., X.W. and J.Q. performed experiments. C.Z., T.D., J.G., X.W. and W.L. analyzed the data and wrote the manuscript. All authors read and approved the manuscript.

Declaration of Competing Interest

The patent concerning the technology presented in this work is applying for.

Acknowledgements

This work was financially supported by the National Natural Science Foundation of China (81973245, 81673361, 81690263 and 81673370), National Postdoctoral Program for Innovative Talent (BX20190086), Shanghai Municipal Commission of Health and Family Planning (2018BR04), Shanghai Natural Science Foundation (19431900300 and 18ZR1404800) and Pudong New Area Commission of Science & Technology (PKJ2016-Y46).

Appendix A. Supplementary data

Supplementary data to this article can be found online at https://doi.org/10.1016/j.jconrel.2020.01.018.

References

[1] R. Langer, Drug delivery and targeting, Nature 392 (1998) 5–10.
[2] T.M. Allen, P.R. Cullis, Drug delivery systems: entering the mainstream, Science 303 (2004) 1818–1822.
[3] M.L. Immordino, F. Dosio, L. Cattel, Stealth liposomes: review of the basic science, rationale, and clinical applications existing and potential, Int. J. Nanomedicine 1 (2006) 297–315.
[4] T.M. Allen, P.R. Cullis, Liposomal drug delivery systems: from concept to clinical applications, Adv. Drug Deliv. Rev. 65 (2013) 36–48.
[5] A. Sharma, U.S. Sharma, Liposomes in drug delivery: progress and limitations, Int. J. Pharm. 154 (1997) 123–140.
[6] A. Prokop, V. Weissig, Intracellular Delivery III: Market Entry Barriers of Nanomedicines, (2016).
[7] D. Papahadjopoulos, T.M. Allen, A. Gabizon, E. Mayhew, K. Matthay, S.K. Huang, K.D. Lee, M.C. Woodle, D.D. Lasic, C. Redemann, Sterically stabilized liposomes: improvements in pharmacokinetics and antitumor therapeutic efficacy, Proc. Natl. Acad. Sci. 88 (1991) 11460.
[8] D.D. Lasic, Doxorubicin in sterically stabilized liposomes, Nature 380 (1996) 561–562.
[9] V.P. Torchilin, Recent advances with liposomes as pharmaceutical carriers, Nat. Rev. Drug Discov. 4 (2005) 145–160.
[10] H. Ando, S. Kobayashi, A.S. Abu Lila, N.E. Eldin, C. Kato, T. Shimizu, M. Ukawa, K. Kawazoe, T. Ishida, Advanced therapeutic approach for the treatment of malignant pleural mesothelioma via the intrapleural administration of liposomal pemetrexed, J. Control. Release 220 (2015) 29–36.
[11] R.J. Lee, P.S. Low, Folate-mediated tumor cell targeting of liposome-entrapped doxorubicin in vitro, Biochim. Biophys. Acta Biomembr. 1233 (1995) 134–144.
[12] P. Sapra, T.M. Allen, Ligand-targeted liposomal anticancer drugs, Prog. Lipid Res. 42 (2003) 439–462.
[13] C. Zhan, C. Li, X. Wei, W. Lu, W. Lu, Toxins and derivatives in molecular pharmaceutics: drug delivery and targeted therapy, Adv. Drug Deliv. Rev. 90 (2015) 101–118.
[14] K. Maruyama, T. Takizawa, T. Yuda, S.J. Kennel, L. Huang, M. Iwatsuru, Targetability of novel immunoliposomes modified with amphipathic poly(ethylene glycol) s conjugated at their distal terminals to monoclonal antibodies, Biochim. Biophys. Acta Biomembr. 1234 (1995) 74–80.
[15] X. Wei, C. Zhan, X. Chen, J. Hou, C. Xie, W. Lu, Retro-Inverso isomer of Angiopep-2:

a stable d-peptide ligand inspires brain-targeted drug delivery, Mol. Pharm. 11 (2014) 3261–3268.
[16] Z. Jiang, J. Guan, J. Qian, C. Zhan, Peptide ligand-mediated targeted drug delivery of nanomedicines, Biomater. Sci. 7 (2019) 461–471.
[17] A. Albanese, P.S. Tang, W.C.W. Chan, The effect of nanoparticle size, shape, and surface chemistry on biological systems, Annu. Rev. Biomed. Eng. 14 (2012) 1–16.
[18] P.P. Karmali, D. Simberg, Interactions of nanoparticles with plasma proteins: implication on clearance and toxicity of drug delivery systems, Expert Opin. Drug Deliv. 8 (2011) 343–357.
[19] A. Salvati, A.S. Pitek, M.P. Monopoli, K. Prapainop, F.B. Bombelli, D.R. Hristov, P.M. Kelly, C. Åberg, E. Mahon, K.A. Dawson, Transferrin-functionalized nanoparticles lose their targeting capabilities when a biomolecule corona adsorbs on the surface, Nat. Nanotechnol. 8 (2013) 137.
[20] S. Behzadi, V. Serpooshan, R. Sakhtianchi, B. Müller, K. Landfester, D. Crespy, M. Mahmoudi, Protein corona change the drug release profile of nanocarriers: the “overlooked” factor at the nanobio interface, Colloids Surf. B: Biointerfaces 123 (2014) 143–149.
[21] S. Zanganeh, R. Spitler, M. Erfanzadeh, A.M. Alkilany, M. Mahmoudi, Protein corona: opportunities and challenges, Int. J. Biochem. Cell Biol. 75 (2016) 143–147.
[22] N. Bertrand, P. Grenier, M. Mahmoudi, E.M. Lima, E.A. Appel, F. Dormont, J.-M. Lim, R. Karnik, R. Langer, O.C. Farokhzad, Mechanistic understanding of in vivo protein corona formation on polymeric nanoparticles and impact on pharmacokinetics, Nat. Commun. 8 (2017) 777.
[23] M. Hadjidemetriou, Z. Al-Ahmady, K. Kostarelos, Time-evolution of in vivo protein corona onto blood-circulating PEGylated liposomal doxorubicin (DOXIL) nanoparticles, Nanoscale 8 (2016) 6948–6957.
[24] M. Hadjidemetriou, S. McAdam, G. Garner, C. Thackeray, D. Knight, D. Smith, Z. Al-Ahmady, M. Mazza, J. Rogan, A. Clamp, K. Kostarelos, The human in vivo biomolecule Corona onto PEGylated liposomes: a proof-of-concept clinical study, Adv. Mater. 31 (2019) 1803335.
[25] M. Lundqvist, J. Stigler, G. Elia, I. Lynch, T. Cedervall, K.A. Dawson, Nanoparticle size and surface properties determine the protein corona with possible implications for biological impacts, Proc. Natl. Acad. Sci. 105 (2008) 14265.
[26] Z. Zhang, J. Guan, Z. Jiang, Y. Yang, J. Liu, W. Hua, Y. Mao, C. Li, W. Lu, J. Qian, C. Zhan, Brain-targeted drug delivery by manipulating protein corona functions, Nat. Commun. 10 (2019) 3561.
[27] P.R. Hansen, A. Oddo, Fmoc solid-phase peptide synthesis, Methods Mol Biol. (Clifton, N.J.) 1348 (2015) 33–50.
[28] X. Han, J. Liu, M. Liu, C. Xie, C. Zhan, B. Gu, Y. Liu, L. Feng, W. Lu, 9-NC-loaded folate-conjugated polymer micelles as tumor targeted drug delivery system: preparation and evaluation in vitro, Int. J. Pharm. 372 (2009) 125–131.
[29] C.B. Hansen, G.Y. Kao, E.H. Moase, S. Zalipsky, T.M. Allen, Attachment of antibodies to sterically stabilized liposomes: evaluation, comparison and optimization of coupling procedures, Biochim. Biophys. Acta Biomembr. 1239 (1995) 133–144.
[30] F. Olson, C.A. Hunt, F.C. Szoka, W.J. Vail, D. Papahadjopoulos, Preparation of liposomes of defined size distribution by extrusion through polycarbonate membranes, Biochim. Biophys. Acta Biomembr. 557 (1979) 9–23.
[31] G. Haran, R. Cohen, L.K. Bar, Y. Barenholz, Transmembrane ammonium sulfate gradients in liposomes produce efficient and stable entrapment of amphipathic weak bases, Biochim. Biophys. Acta Biomembr. 1151 (1993) 201–215.
[32] G.R. Bartlett, Phosphorus assay in column chromatography, J. Biol. Chem. 234 (1959) 466–468.
[33] X. Wei, C. Zhan, Q. Shen, W. Fu, C. Xie, J. Gao, C. Peng, P. Zheng, W. Lu, A D-peptide ligand of nicotine acetylcholine receptors for brain-targeted drug delivery, Angew. Chem. Int. Ed. 54 (2015) 3023–3027.
[34] C. Zhan, B. Li, L. Hu, X. Wei, L. Feng, W. Fu, W. Lu, Micelle-based brain-targeted drug delivery enabled by a nicotine acetylcholine receptor ligand, Angew. Chem. Int. Ed. 50 (2011) 5482–5485.
[35] J. Guan, Q. Shen, Z. Zhang, Z. Jiang, Y. Yang, M. Lou, J. Qian, W. Lu, C. Zhan, Enhanced immunocompatibility of ligand-targeted liposomes by attenuating natural IgM absorption, Nat. Commun. 9 (2018) 2982.
[36] J. Guan, Z. Jiang, M. Wang, Y. Liu, J. Liu, Y. Yang, T. Ding, W. Lu, C. Gao, J. Qian, C. Zhan, Short peptide-mediated brain-targeted drug delivery with enhanced immunocompatibility, Mol. Pharm. 16 (2019) 907–913.
[37] E.T. Dams, P. Laverman, W.J. Oyen, G. Storm, G.L. Scherphof, J.W. van Der Meer, F.H. Corstens, O.C. Boerman, Accelerated blood clearance and altered biodistribution of repeated injections of sterically stabilized liposomes, J. Pharmacol. Exp. Ther. 292 (2000) 1071–1079.
[38] T. Ishida, H. Kiwada, Accelerated blood clearance (ABC) phenomenon upon repeated injection of PEGylated liposomes, Int. J. Pharm. 354 (2008) 56–62.
[39] T. Ishida, M. Ichihara, X. Wang, H. Kiwada, Spleen plays an important role in the induction of accelerated blood clearance of PEGylated liposomes, J. Control. Release 115 (2006) 243–250.
[40] X. Wang, T. Ishida, H. Kiwada, Anti-PEG IgM elicited by injection of liposomes is involved in the enhanced blood clearance of a subsequent dose of PEGylated liposomes, J. Control. Release 119 (2007) 236–244.
[41] D. Ricklin, G. Hajishengallis, K. Yang, J.D. Lambris, Complement: a key system for immune surveillance and homeostasis, Nat. Immunol. 11 (2010) 785.
[42] M.R. Ehrenstein, C.A. Notley, The importance of natural IgM: scavenger, protector and regulator, Nat. Rev. Immunol. 10 (2010) 778.
[43] T. Ishida, H. Harashima, H. Kiwada, Liposome clearance, Biosci. Rep. 22 (2002) 197.
[44] V.P. Vu, G.B. Gifford, F. Chen, H. Benasutti, G. Wang, E.V. Groman, R. Scheinman, L. Saba, S.M. Moghimi, D. Simberg, Immunoglobulin deposition on biomolecule corona determines complement opsonization efficiency of preclinical and clinical nanoparticles, Nat. Nanotechnol. 14 (2019) 260–268.
[45] P. Saeyoung, M.H. Nahm, %J Infection, Immunity, Older Adults Have A Low Capacity To Opsonize Pneumococci due to Low IgM Antibody Response to Pneumococcal Vaccinations, 79 (2011), pp. 314–320.
[46] S.V. Kaveri, G.J. Silverman, B.J.J.O.I. Jagadeesh, Natural IgM in Immune Equilibrium and Harnessing Their Therapeutic Potential, 188 (2012), pp. 939–945.
[47] M.J. Walport, Complement, N. Engl. J. Med. 344 (2001) 1058–1066.
[48] A.M. Blom, B.O. Villoutreix, B.J.M.I. Dahlbäck, Complement Inhibitor C4b-Binding Protein—Friend Or Foe In The Innate Immune System? 40 (2004), pp. 1333–1346.
[49] J.V. Sarma, P.A. Ward, The complement system, Cell Tissue Res. 343 (2011) 227–235.
[50] X. Wang, H. Wang, K. Jiang, Y. Zhang, C. Zhan, M. Ying, M. Zhang, L. Lu, R. Wang, S. Wang, D.J. Burgess, H. Wang, W. Lu, Liposomes with cyclic RGD peptide motif triggers acute immune response in mice, J. Control. Release 293 (2019) 201–214.
[51] M.S. Diamond, B. Shrestha, A. Marri, D. Mahan, M. Engle, B Cells and antibody play critical roles in the immediate defense of disseminated infection by west nile encephalitis virus, J. Virol. 77 (2003) 2578–2586.
[52] R.J. Lee, P.S. Low, Delivery of liposomes into cultured kb cells via folate receptor-mediated endocytosis, J. Biol. Chem. 269 (1994) 3198–3204.
[53] J. Sudimack, R.J. Lee, Targeted drug delivery via the folate receptor, Adv. Drug Deliv. Rev. 41 (2000) 147–162.
[54] K. Shroff, E. Kokkoli, PEGylated liposomal doxorubicin targeted to α5β1-expressing MDA-MB-231 breast cancer cells, Langmuir 28 (2012) 4729–4736.
[55] A. Garg, A.W. Tisdale, E. Haidari, E. Kokkoli, Targeting colon cancer cells using PEGylated liposomes modified with a fibronectin-mimetic peptide, Int. J. Pharm. 366 (2009) 201–210.
[56] X. Sun, Z. Pang, H. Ye, B. Qiu, L. Guo, J. Li, J. Ren, Y. Qian, Q. Zhang, J. Chen, X. Jiang, Co-delivery of pEGFP-hTRAIL and paclitaxel to brain glioma mediated by an angiopep-conjugated liposome, Biomaterials 33 (2012) 916–924.
[57] X. Tian, S. Nyberg, P.S. Sharp, J. Madsen, N. Daneshpour, S.P. Armes, J. Berwick, M. Azzouz, P. Shaw, N.J. Abbott, G. Battaglia, LRP-1-mediated intracellular antibody delivery to the central nervous system, Sci. Rep. 5 (2015) 11990.
[58] M. Ying, Q. Shen, Y. Liu, Z. Yan, X. Wei, C. Zhan, J. Gao, C. Xie, B. Yao, W. Lu, Stabilized heptapeptide A7R for enhanced multifunctional liposome-based tumor-targeted drug delivery, ACS Appl. Mater. Interfaces 8 (2016) 13232–13241.
[59] J. Cao, R. Wang, N. Gao, M. Li, X. Tian, W. Yang, Y. Ruan, C. Zhou, G. Wang, X. Liu, S. Tang, Y. Yu, Y. Liu, G. Sun, H. Peng, Q. Wang, A7RC peptide modified paclitaxel liposomes dually target breast cancer, Biomater. Sci. 3 (2015) 1545–1554.
[60] Y. Vachutinsky, M. Oba, K. Miyata, S. Hiki, M.R. Kano, N. Nishiyama, H. Koyama, K. Miyazono, K. Kataoka, Antiangiogenic gene therapy of experimental pancreatic tumor by sFlt-1 plasmid DNA carried by RGD-modified crosslinked polyplex micelles, J. Control. Release 149 (2011) 51–57.
[61] W.J. Kim, J.W. Yockman, J.H. Jeong, L.V. Christensen, M. Lee, Y.-H. Kim, S.W. Kim, Anti-angiogenic inhibition of tumor growth by systemic delivery of PEI-g-PEG-RGD/pCMV-sFlt-1 complexes in tumor-bearing mice, J. Control. Release 114 (2006) 381–388.
[62] J.-A. Park, Y.J. Lee, J.W. Lee, K.C. Lee, G.I. An, K.M. Kim, B.I. Kim, T.-J. Kim, J.Y. Kim, Cyclic RGD peptides incorporating cycloalkanes: synthesis and evaluation as PET radiotracers for tumor imaging, ACS Med. Chem. Lett. 5 (2014) 979–982.
[63] K. Chen, J. Xie, X. Chen, RGD-human serum albumin conjugates as efficient tumor targeting probes, Mol. Imaging 8 (2009) 65–73.
[64] F. Danhier, B. Vroman, N. Lecouturier, N. Crokart, V. Pourcelle, H. Freichels, C. Jérôme, J. Marchand-Brynaert, O. Feron, V. Préat, Targeting of tumor endothelium by RGD-grafted PLGA-nanoparticles loaded with paclitaxel, J. Control. Release 140 (2009) 166–173.
[65] M. Scatena, M. Almeida, M.L. Chaisson, N. Fausto, R.F. Nicosia, C.M. Giachelli, NF-kappaB mediates alphavbeta3 integrin-induced endothelial cell survival, J. Cell Biol. 141 (1998) 1083–1093.
[66] R. Evans, I. Patzak, L. Svensson, K. De Filippo, K. Jones, A. McDowall, N. Hogg, Integrins in immunity, J. Cell Sci. 122 (2009) 215.
[67] E. Ruoslahti, Integrins, J. Clin. Invest. 87 (1991) 1–5.
[68] J. Qin, D. Chen, H. Hu, Q. Cui, M. Qiao, B. Chen, Surface modification of RGD-liposomes for selective drug delivery to monocytes/neutrophils in brain, Chem. Pharm. Bull. 55 (2007) 1192–1197.
[69] S. Jain, V. Mishra, P. Singh, P.K. Dubey, D.K. Saraf, S.P. Vyas, RGD-anchored magnetic liposomes for monocytes/neutrophils-mediated brain targeting, Int. J. Pharm. 261 (2003) 43–55.
[70] G.A. Koning, R.M. Schiffelers, M.H.M. Wauben, R.J. Kok, E. Mastrobattista, G. Molema, T.L.M. ten Hagen, G. Storm, Targeting of angiogenic endothelial cells at sites of inflammation by dexamethasone phosphate–containing RGD peptide liposomes inhibits experimental arthritis, Arthritis Rheum. 54 (2006) 1198–1208.
[71] M. Mahmoudi, Debugging Nano–bio interfaces: systematic strategies to accelerate clinical translation of nanotechnologies, Trends Biotechnol. 36 (2018) 755–769.
[72] L.K. Müller, J. Simon, C. Rosenauer, V. Mailänder, S. Morsbach, K. Landfester, The transferability from animal models to humans: challenges regarding aggregation and protein Corona formation of nanoparticles, Biomacromolecules 19 (2018) 374–385.
[73] S. Milani, F. Baldelli Bombelli, A.S. Pitek, K.A. Dawson, J. Rädler, Reversible versus irreversible binding of transferrin to polystyrene nanoparticles: soft and hard corona, ACS Nano 6 (2012) 2532–2541.
[74] A. Chanan-Khan, J. Szebeni, S. Savay, L. Liebes, N.M. Rafique, C.R. Alving, F.M. Muggia, Complement activation following first exposure to pegylated liposomal doxorubicin (Doxil®): possible role in hypersensitivity reactions, Ann. Oncol. 14 (2003) 1430–1437.
[75] F. Meunier, H.G. Prentice, O. Ringdén, Liposomal amphotericin B (AmBisome): safety data from a phase II/III clinical trial, J. Antimicrob. Chemother. 28 (1991) 83–91.

[76] I. Lynch, K.A. Dawson, Protein-nanoparticle interactions, Nano Today 3 (2008) 40–47.
[77] L. Vroman, A.L. Adams, G.C. Fischer, P.C. Munoz, Interaction of high molecular-weight Kininogen, factor-xii, and fibrinogen in plasma at interfaces, Blood 55 (1980) 156–159.
[78] V.H. Nguyen, B.-J. Lee, Protein corona: a new approach for nanomedicine design, Int. J. Nanomedicine 12 (2017) 3137–3151.
[79] A.L. Barrán-Berdón, D. Pozzi, G. Caracciolo, A.L. Capriotti, G. Caruso, C. Cavaliere, A. Riccioli, S. Palchetti, A. Laganà, Time evolution of nanoparticle–protein Corona in human plasma: relevance for targeted drug delivery, Langmuir 29 (2013) 6485–6494.
[80] A. Bigdeli, S. Palchetti, D. Pozzi, M.R. Hormozi-Nezhad, F. Baldelli Bombelli, G. Caracciolo, M. Mahmoudi, Exploring cellular interactions of liposomes using protein Corona fingerprints and physicochemical properties, ACS Nano 10 (2016) 3723–3737.
[81] S. Palchetti, V. Colapicchioni, L. Digiacomo, G. Caracciolo, D. Pozzi, A.L. Capriotti, G. La Barbera, A. Laganà, The protein corona of circulating PEGylated liposomes, Biochim. Biophys. Acta Biomembr. 1858 (2016) 189–196.
[82] M.P. Monopoli, D. Walczyk, A. Campbell, G. Elia, I. Lynch, F. Baldelli Bombelli, K.A. Dawson, Physical – chemical aspects of protein corona: relevance to in vitro and in vivo biological impacts of nanoparticles, J. Am. Chem. Soc. 133 (2011) 2525–2534.